Progress In Electromagnetics Research B, Vol. 56, 269–287, 2013

PERMANENT MAGNET THRUST BEARING: THEORETICAL AND EXPERIMENTAL RESULTS

Siddappa I. Bekinal[1, *], Tumkur R. Anil[1], Soumendu Jana[2], Sadanand S. Kulkarni[2], Aditya Sawant[1], Narsinha Patil[1], and Sagar Dhond[1]

[1]Department of Mechanical Engineering, Gogte Institute of Technology, Belgaum 590008, Karnataka, India

[2]Propulsion Division, National Aerospace Laboratories, Bangalore 560017, Karnataka, India

Abstract—This paper presents the design and analysis of permanent magnet (PM) thrust bearing made up of three ring pairs for five degrees of freedom of the inner rings (rotor rings). The arrangement pattern of rings in PM bearing is considered in two ways: conventional structure and Halbach structure. The simplified three dimensional (3D) mathematical models employing Coulombian approach and vector method are used to design the bearing. MATLAB codes are written to evaluate the axial force, stiffness and moments in both the structures for five degrees of freedom, thereby the effect of axial, radial and angular displacements of the rotor on the aforementioned characteristics is addressed. The results of the mathematical model are validated by the results of 3D Finite Element Analysis (FEA) and experiments. It is observed that, the conventional structure seems to be more sensitive to the angular displacement, as the percentage decrease in force and stiffness is more with respect to angular displacement than the Halbach structure. The effect of angular displacement of the rotor on the performance of bearing in both the structures is crucial.

1. INTRODUCTION

The most suitable solution to improve the system efficiency in high-speed applications is by the utilization of the contact free feature of magnetic and foil bearings. There are mainly two types of magnetic bearings: active and passive magnetic bearings. The passive magnetic

Received 16 October 2013, Accepted 5 November 2013, Scheduled 8 November 2013

* Corresponding author: Siddappa Iranna Bekinal (sibekinal@git.edu).

bearings do not need any sensors and electronic equipments for control and extra input energy, so they are compact and suitable to use. The possible ways to achieve passive magnetic bearings are by using superconductors, diamagnetic, eddy current effect and permanent magnets. The simplest type of passive magnetic bearing is the structure consisting of only permanent magnets. PM bearings are magneto-mechanical elements and they offer relative motion between the moving parts without any physical contact by utilizing the attractive or repulsive forces generated between the magnets. The suitable characteristics (no lubrication, no maintenance, no power and no input energy etc.) of PM bearings made of ring magnets are utilized in many applications such as energy storage flywheels, turbo molecular pumps, hard disk drive spindle motors, moment gyro applications and conveyor systems [1–5]. The load carrying capacity (force) and stiffness are the most important design features in PM bearings. The analytical method, FEA and the experimental design methods are the possible options to optimize the features. The analytical approach is the most promising and fastest technique as compared to other two.

The two dimensional (2D) and 3D analytical design relationships for force and stiffness in PM bearings were presented by the many researchers either by using Lorentzian or by Coulombian approach. In presenting 2D and 3D analytical equations, authors [6–14] have considered the concentric ring magnets, which might not be prevailing in actual scenario. Secondly, the analytical expressions involve elliptical integrals or special functions that are tedious while dealing with more than one degree of freedom of the rotor magnet. In [15], Paden et al. have presented 2D analytical equations for force and stiffness as a function of radial displacement of the rotor in axially magnetized PM bearing but the radial displacement effect on the rotor performance was not addressed. The authors in [16] presented 3D analytical equations for force in axially magnetized radial bearings by considering the eccentric rings but the effect of eccentricity on the rotor performance was not presented. Another aspect is that, till date, the researchers have not addressed the effect of radial and angular displacements of a rotor on force and stiffness (only the effect of axial offset was considered) in permanent magnet bearings with perpendicular polarizations. Bekinal et al. [17–20] have presented the simplified 3D mathematical models for force and stiffness in axial and radial polarized PM bearings made of non-concentric ring magnets. This paper presents the design, analysis and development of PM thrust bearing made of three ring pairs for five degrees of freedom of the rotor (three translational x, y and z and two angular ξ and γ). The arrangement pattern of rings is considered in two ways. One

of them is a conventional axial array as shown in Fig. 1(a), wherein the axially polarized rings are arranged in opposition. Second, the Halbach structure as shown in Fig. 1(b), wherein the rings are arranged in rotating magnetization pattern. The accuracy of the analytical design equations is validated by the results of 3D FEA in ANSYS and experiments.

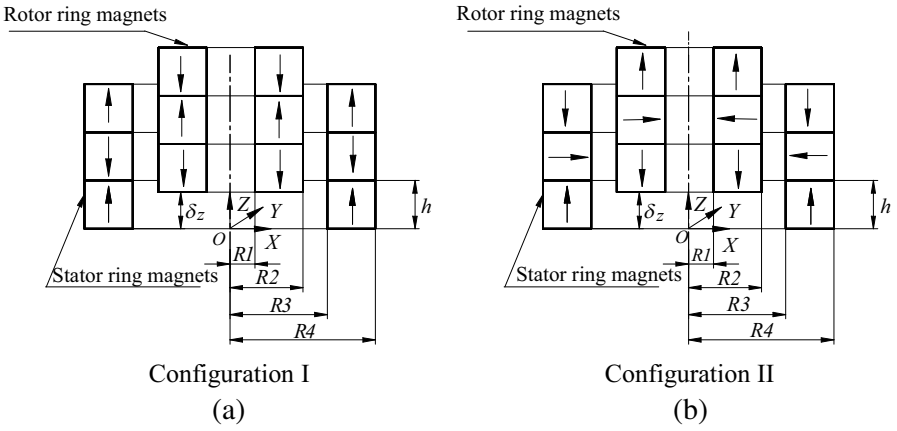

Figure 1. Configurations of PM thrust bearing. (a) Conventional axially stacked structure. (b) Halbach structure.

2. PERMANENT MAGNET THRUST BEARING CONFIGURATIONS

Two configurations of PM thrust bearing are shown in Fig. 1. Each configuration consists of three sets of PM ring pairs. At first, rings are polarized axially and arranged in opposition (Fig. 1(a)), whereas rings are perpendicularly polarized in second and constitute the Halbach structure (Fig. 1(b)). The configurations act as radial and axial bearings depending upon the relative axial offset of the inner rings set with respect to the outer. They generate positive axial force when axial offset is negative and vice versa. The axial stiffness of the configurations is maximum when there is no relative axial displacement of the inner rings with respect to the outer.

3. DESIGN AND ANALYSIS OF PERMANENT MAGNET THRUST BEARING

3.1. Mathematical Models

Simplified 3D mathematical models to determine the force, stiffness and moment in axial [17, 18] and radial [19, 20] polarized PM bearings were presented by Bekinal et al. for non-concentric ring magnets using Coulombian and vector approaches. The mathematical model of perpendicularly polarized PM bearing is presented in this paper for non-concentric ring magnets. The basic configuration of a PM bearing with perpendicularly polarized rings is shown in Fig. 2.

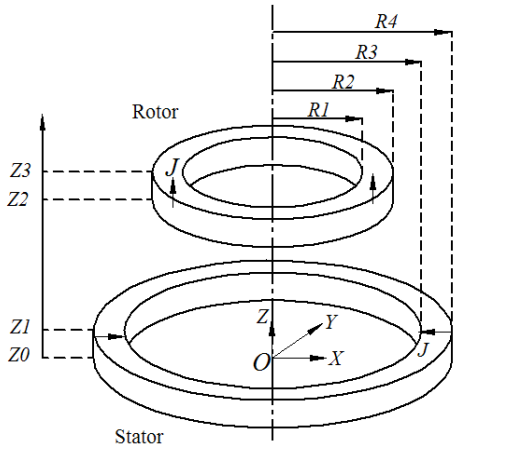

Figure 2. Configuration of a PM bearing with perpendicular polarizations.

The inner and outer radii of the inner permanent magnet ring are $R1$ and $R2$ respectively, $R3$ and $R4$ are of outer ring. The thicknesses of the outer and inner magnets are $Z1 - Z0 = h$ and $Z3 - Z2 = h$ respectively. Magnetic polarization 'J' of outer magnet is perpendicular to the inner one as depicted by Fig. 2. There are magnetic forces of attraction and repulsion between the charged surfaces of the rotor and stator magnet. In order to calculate these forces the rotor and stator magnet surfaces are divided into a large number of finite surface elements. The net force acting on the rotor magnet is calculated by calculating the forces between elemental surfaces of the rotor and stator magnets. The important step in the force calculation involves calculation of coordinates of the surface

elements for assumed rotor displacement in five degrees of freedom. Initially, the rotor magnet is displaced from its nominal position by an arbitrary distance of '**e**' enabling three translational movements in XYZ coordinate system as shown in Fig. 3. Co-ordinate of the surface elements of the displaced rotor as well as stator can be calculated from appropriate geometric consideration.

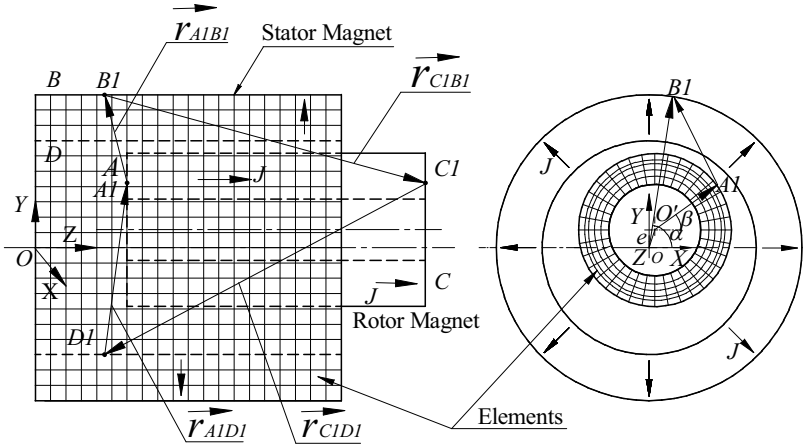

Figure 3. Arrangement of rotor and stator magnets with respect to translational degrees of freedom (x, y and z).

In the next step, the rotor is rotated with an arbitrary angular displacement of ξ about X-axis as shown in Fig. 4 in the anticlockwise direction (positive rotation). The coordinates of surface elements at new position of the rotor are determined based on geometric consideration. Similarly, rotation about Y-axis (γ) can also be considered. Due to the symmetry of the rings, the effect of angular displacements ξ and γ on bearing characteristics remains similar.

The general procedure followed in developing the mathematical model of perpendicularly polarized PM bearing is same as that of the mathematical model of axial [18] and radial [19, 20] polarized bearings except the coordinate positions of the elements on the stator and rotor magnet surfaces. In this regard, only general coordinate positions of the elements on the rotor and stator surfaces are presented in this section and general equations of the mathematical model are presented in the appendix A.

The positions of the elements $A1$ and $B1$ in terms of mean radius, equivalent radial distance, mean distance from the respective centers

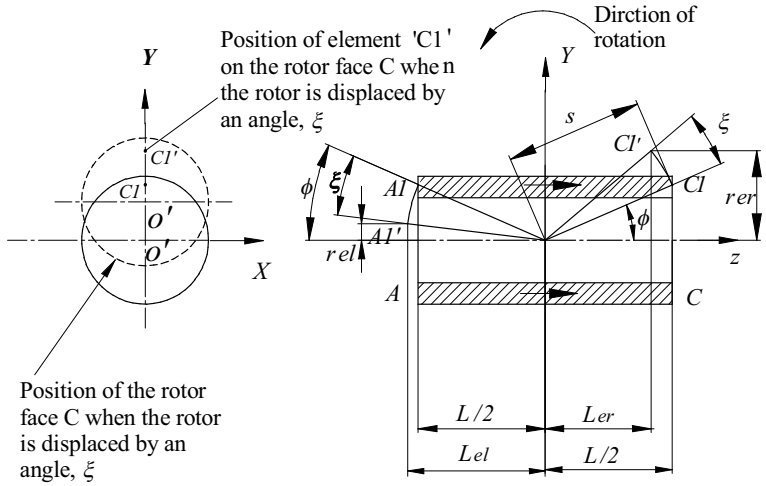

Figure 4. Positions of rotor with elements on the magnet faces A and C and with an angular displacement 'ξ' about X-axis in the anticlockwise direction [18].

and the angles α, β, ϕ and ξ can be expressed as,

$$\begin{aligned}
&s = \sqrt{(0.5L)^2 + (r_{A1M}\sin(\beta))^2} && \tan(\phi) = \frac{r_{A1M}\sin(\beta)}{0.5L} \\
&r_{el} = s\sin(\phi - \xi) && r_{er} = s\sin(\phi + \xi) \\
&L_{el} = s\cos(\phi - \xi) && L_{er} = s\cos(\phi + \xi) \\
&\vec{X}_{A1} = (x + r_{A1M}\cos(\beta))\,\mathbf{i} && \vec{X}_{B1} = (R4\cos(\alpha))\,\mathbf{i} \\
&\vec{Y}_{A1} = (y + r_{el})\,\mathbf{j} && \vec{Y}_{B1} = (R4\sin(\alpha))\,\mathbf{j} \\
&\vec{Z}_{A1} = (z - (L_{el} - 0.5L))\,\mathbf{k} && \vec{Z}_{B1} = (L_{B1M})\,\mathbf{k}
\end{aligned} \tag{1}$$

where, angles α and β are referred in XY plane (Fig. 3), and ϕ and ξ are in YZ plane (Fig. 4). r_{A1M} is the mean radius of element $A1$ from inner magnet centre 'O'', L_{B1M} the mean axial distance (parallel to Z-axis) of element $B1$ from outer magnet centre 'O', $R4$ the outer radius of the outer ring, r_{el} the equivalent vertical distance (parallel to Y-axis) of element $A1$ from the axis of stator magnet, and L_{el} an equivalent axial distance of element $A1$ from the centre of the magnet in Z direction.

The positions of the elements $C1$ and $D1$ in terms of mean radius, equivalent radial distance, mean distance from the respective centers

and the angles α, β, ϕ and ξ can be expressed as:

$$\begin{aligned} \vec{X}_{C1} &= (x + r_{C1M}\cos(\beta))\,\mathbf{i} & \vec{X}_{D1} &= (R3\cos(\alpha))\,\mathbf{i} \\ \vec{Y}_{C1} &= (y + r_{er})\,\mathbf{j} & \vec{Y}_{D1} &= (R3\sin(\alpha))\,\mathbf{j} \\ \vec{Z}_{C1} &= (z - (L_{el} - 0.5L) + L_{el} + L_{er})\,\mathbf{k} & \vec{Z}_{D1} &= (L_{D1M})\,\mathbf{k} \end{aligned} \quad (2)$$

where, L_{er} is an equivalent axial distance of element $C1$ from the centre of the magnet in the Z direction, and L_{D1M} is the mean axial distance (parallel to Z-axis) of element $D1$ from outer magnet centre 'O'.

3.2. Analysis of PM Thrust Bearing using Mathematical Models

In the present work, N35 Nd-Fe-B magnet rings ($Br = 1.2\,\mathrm{T}$) with geometrical dimensions given in Table 1 are selected for the analysis.

The variations of axial force with axial offset at different radial and angular displacements of the rotor in configurations I and II are

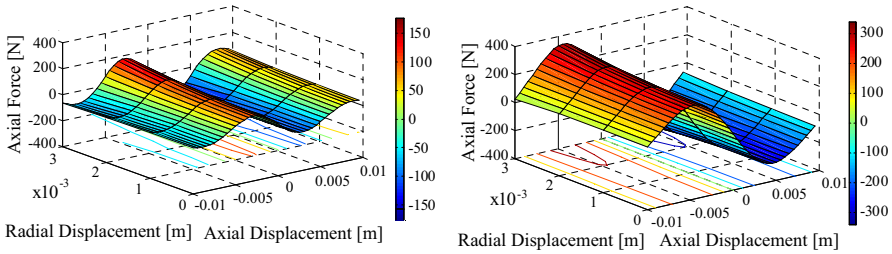

Figure 5. Variations of axial force with axial offset for different radial displacements of the rotor. (a) Configuration I. (b) Configuration II.

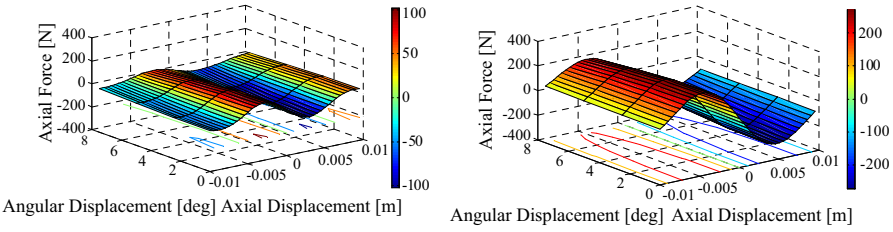

Figure 6. Variations of axial force with axial offset for different angular displacements of the rotor. (a) Configuration I. (b) Configuration II.

Table 1. Geometrical dimensions of the ring magnets.

	Inner ring dimensions	Outer ring dimensions
Inner radius [mm]	$R1 = 20$	$R3 = 29$
Outer radius [mm]	$R2 = 25$	$R4 = 34$
Thickness, h [mm]	$Z1 - Z0 = 5$	$Z3 - Z2 = 5$

presented in Figs. 5 and 6. The axial force (271.2 N at 5 mm axial offset) generated by the Halbach structure (configuration II) is on the higher side as compared to the conventional structure (configuration I) (101.95 N at 3 mm axial offset) for the same magnet volume at 0 mm radial displacement. The axial force increases with an increase in the radial displacement, whereas it decreases with an increase in the angular displacement in both the configurations.

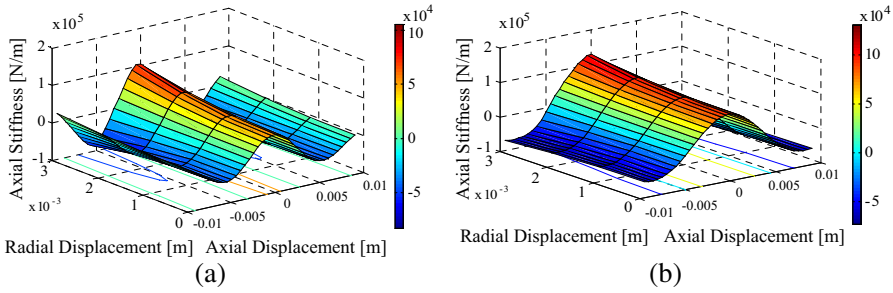

Figure 7. Variations of axial stiffness with axial offset at radial displacements of the rotor. (a) Configuration I. (b) Configuration II.

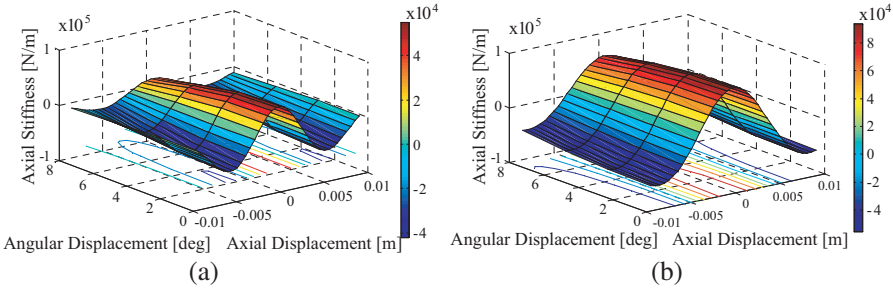

Figure 8. Variations of axial stiffness with axial offset at different angular displacements of the rotor. (a) Configuration I. (b) Configuration II.

Figures 7 and 8 show the variations of axial stiffness with axial offset at different radial and angular displacements of the rotor in configurations I and II. Axial stiffness (93820 N/m at 0 mm axial offset) of the configuration II is higher as compared to the stiffness (55091 N/m at 0 mm axial offset) of the configuration I at 0 mm radial displacement.

Axial stiffness increases with radial displacement and decreases with angular displacement of the rotor. Moments acting on the rotor as a result of radial and angular displacements are calculated at its various axial positions and results are plotted in Figs. 9 and 10. Radial displacement of the rotor in X-axis causes the moment about Y-axis and angular displacement about X-axis causes the moment about the X-axis.

The net moment acting on the rotor is zero when it is concentric with the stator. The magnitude of the moment acting on the rotor due to radial displacements is on the higher side as compared to moment due to angular displacement about the X-axis. The maximum moment acting on the rotor about Y-axis at 3 mm radial displacement

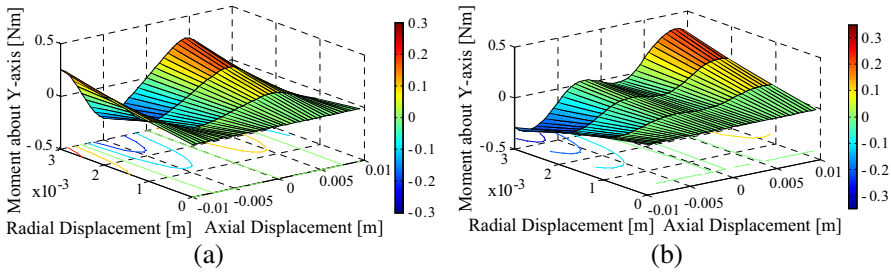

Figure 9. Variations of moment on the rotor due to radial displacements. (a) Configuration I. (b) Configuration II.

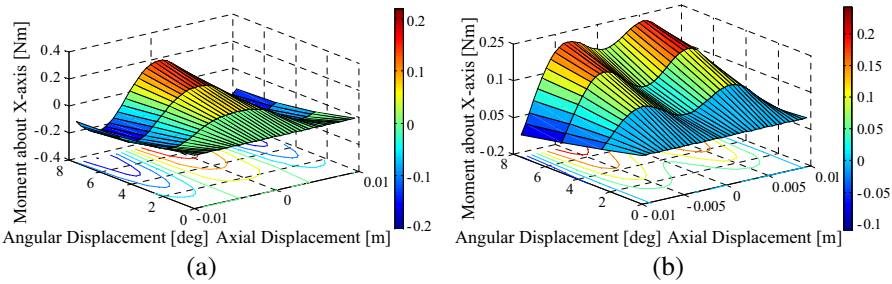

Figure 10. Variations of moment on the rotor due to angular displacements. (a) Configuration I. (b) Configuration II.

in configuration II (0.35 Nm) is higher as compared maximum moment (0.30 Nm) in the configuration I.

3.3. Finite Element Analysis (FEA) of Permanent Magnet Thrust Bearing

3.3.1. Finite Element Modeling of Conventional Structure

The conventional structure was modeled in ANSYS as shown in Fig. 11(a). The local elemental coordinate system is used to define the polarization direction of axial magnetized rings in bearing. The model is analysed with 292338 number of solid 97 type elements having 69037 nodes for five degrees of freedom of the rotor using a magnetic virtual work approach. The properties of the magnetic material selected for the analysis are: $B_r = 1.2\,\mathrm{T}$, $H_c = 868\,\mathrm{kA/m}$ and $\mu_r = 1.1$. The axial force exerted by the outer rings set on the inner one is determined by the movement of inner rings set (rotor rings) in axial, radial and angular directions (Fig. 11(b)).

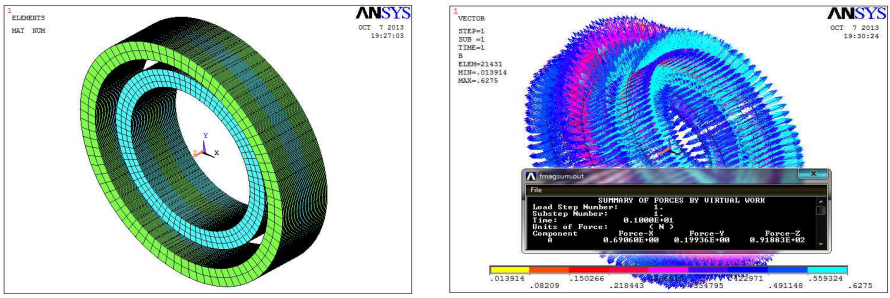

(a) (b)

Figure 11. Finite element analysis of permanent magnet thrust bearing in ANSYS. (a) Finite element model. (b) Axial force exerted by the outer rings set on the inner.

3.3.2. Finite Element Modeling of Halbach Structure

Finite element model of the Halbach structure created in ANSYS is shown in Fig. 12(a). Since the Halbach structure consists of both radial and axial magnetized rings, defining of polarization directions of rings is difficult task. The polarization direction of axial magnetized rings is defined by considering local elemental coordinate system and the elemental coordinate system is rotated to define the polarization direction of radial magnetized rings. For the analysis of the model, 319497 number of solid 97 type elements having 73663 nodes are used.

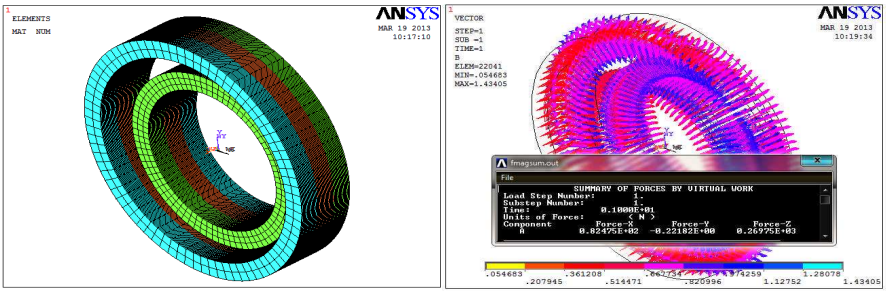

(a) (b)

Figure 12. Finite element analysis of permanent magnet thrust bearing in ANSYS. (a) Finite element model. (b) Axial force exerted by the outer rings set on the inner.

The properties of the magnetic material selected for the analysis are: $B_r = 1.2\,\mathrm{T}$, $H_c = 868\,\mathrm{kA/m}$ and $\mu_r = 1.1$. The axial force exerted by the outer rings set on the inner one is determined by the movement of inner rings set (rotor rings) in axial, radial and angular directions (Fig. 12(b)).

3.3.3. FEA Results

The variations of axial force with axial offset of the rotor for its different radial and angular displacements in configurations I and II are presented in Figs. 13 and 14.

The results shown in Figs. 5, 6, 13 and 14 demonstrate that the results of FEA match closely with the mathematical model results obtained in the previous section for both the configurations. The discrepancy in the results is less than 11% in the configuration I and 5% in configuration II.

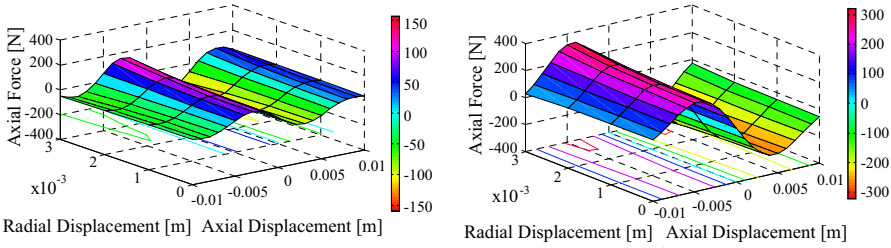

(a) (b)

Figure 13. Variations of axial force with axial offset at different radial displacements of the rotor using FEA in ANSYS. (a) Configuration I. (b) Configuration II.

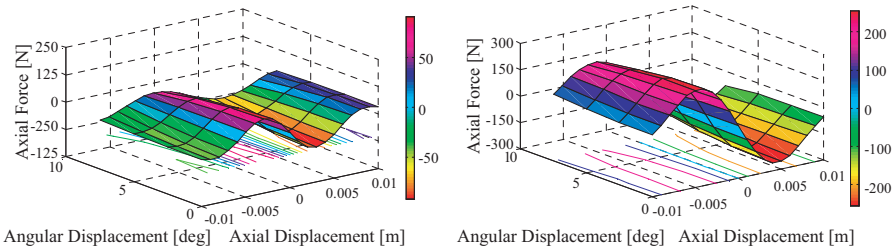

Figure 14. Variations of axial force with axial offset at different angular displacements of the rotor using FEA in ANSYS. (a) Configuration I. (b) Configuration II.

4. EXPERIMENTAL VALIDATION

4.1. Details of Test Rig

A test rig that is designed and fabricated is shown in Figs. 15 and 16. The inner ring holder carries the inner rings set and the outer rings are fitted to the outer ring holder (details of the magnet rings are given in Subsection 3.2). Three axially polarized permanent magnet rings are provided on both inner and outer ring holders to form a configuration I. Two axially polarized rings (Fig. 17(a)) and one radially polarized

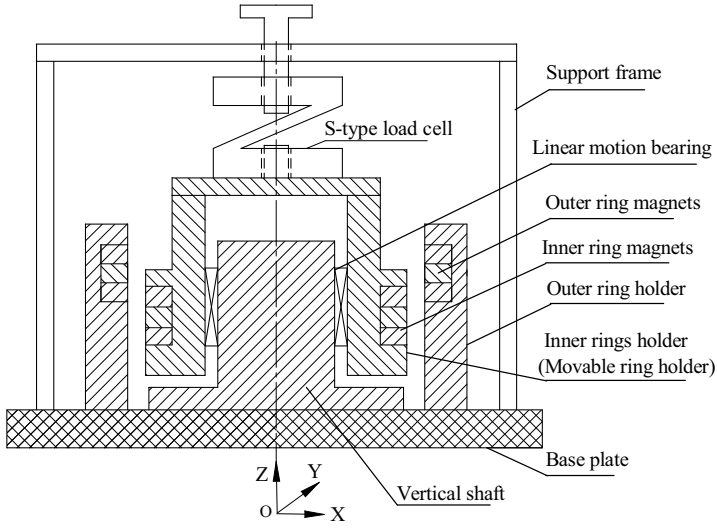

Figure 15. Schematic representation of a test rig.

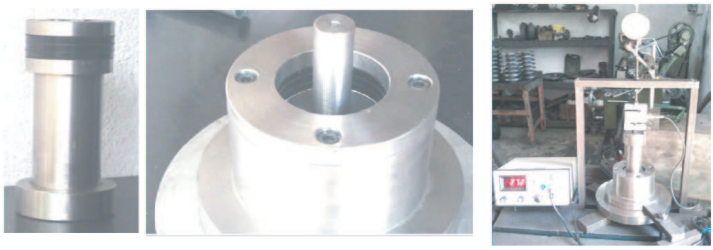

(a) (b) (c)

Figure 16. Details of test rig for the measurement of axial force. (a) Arrangement of rings on the inner ring holder (rotor). (b) Arrangement of rings on the outer ring holder (stator). (c) Test rig with load cell and dial gauge.

(a) (b) (c)

Figure 17. Radial polarized permanent magnet sectors. (a) Axially polarized ring magnets. (b) 45° sectors. (c) 60° sectors.

ring comprising of six sectors each of 60° (Fig. 17(c)) are provided on the inner rings holder and the outer rings holder is provided with one radially polarized ring comprising of eight sectors each of 45° (Fig. 17(b)) and two axially polarized rings to form a configuration II. The ring and sector magnets are fitted to inner and outer ring holders in the required configurations with a great difficulty. Special fixtures as shown Fig. 18 are used to arrange the magnets in the form of required configurations. The linear motion bearing is provided between the inner ring holder and the vertical shaft. The inner ring holder can move in the axial direction with the linear motion bearing and the radial displacement of which is achieved by displacing the vertical shaft radial direction by using a suitable base plate.

The S-type load cell fitted between the inner ring holder and the support frame is used to measure the axial force exerted by the outer rings set on the inner for axial displacements of the rotor. The dial gauge is used to record the axial displacements of the inner rings set. The rotor rings are displaced by 2 mm in the radial direction with respect to the outer rings by providing suitable base plate.

Figure 18. Fixtures for arranging the ring and sector magnets.

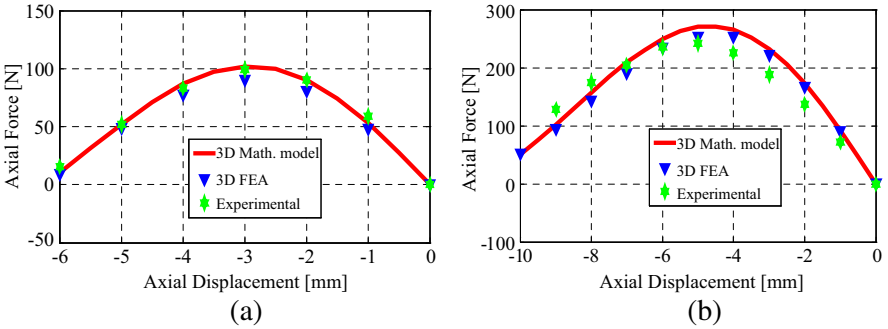

Figure 19. Results of an axial force at 0 mm radial offset. (a) Configuration I. (b) Configuration II.

4.2. Experimental Results

The variations of experimentally measured axial force with axial displacements of the rotor along with the results of 3D FEA and mathematical model in both the configurations (Fig. 1) are shown in Figs. 19 and 20.

The maximum axial force (241.32 N at 5 mm axial offset) generated by the Halbach structure (configuration II) is on the higher side as compared to the conventional structure (configuration I) (99 N at 3 mm axial offset) for the same magnet volume at 0 mm radial displacement. It is also observed that the maximum axial force (117.72 N at 2 mm radial displacement) is on the higher side as compared to the maximum axial force (99 N at 0 mm radial displacement) in the configuration I at 3 mm axial offset. The same character holds good for the configuration II (266.83 N at 2 mm radial displacement and 241.32 N at 0 mm radial displacement) at 5 mm axial offset.

The deviation of experimentally measured results with respect to 3D FEA is less than 2% in the configuration I and 6% in

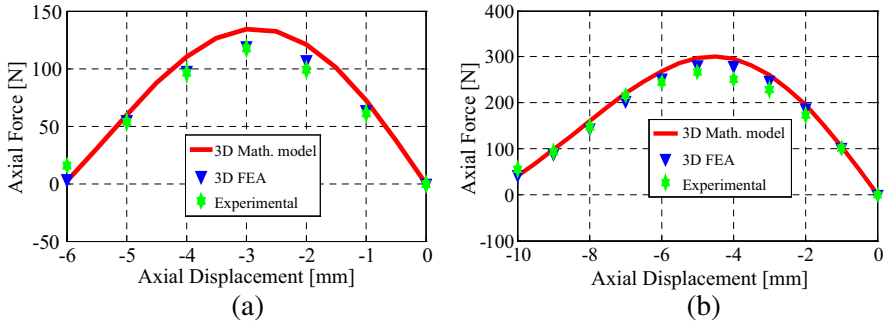

Figure 20. Results of an axial force at 2 mm radial offset. (a) Configuration I. (b) Configuration II.

configuration II. The deviation with respect to mathematical model is less than 12.5% in the configuration I and 11.5% in configuration II. The mismatch between the results might be due to the nonuniform magnetization of the rings, friction between the vertical shaft and linear motion bearing, eccentricity and angular tilt of inner rings with respect to the outer rings etc.

5. CONCLUSIONS

The PM thrust bearing made up of three ring pairs is designed using 3D mathematical models for five degrees of freedom of the rotor rings. In addition, 3D FEA of the bearing using ANSYS is presented. Experiments are conducted to measure the axial force at different axial positions of the inner rings set at 0 and 2 mm radial displacements in both the configurations. The results of the mathematical model are in good agreement with 3D FEA and experimental results. The axial force and stiffness increase with the radial displacement of the inner rings set and decrease with the angular displacement in both the configurations. The effect of angular displacement on the bearing characteristics is crucial. It is observed that, the Halbach structure would be the best possible choice between the two structures as it generates greater axial force and stiffness for the same magnet volume and seems to be less sensitive to the angular displacement (percentage decrease in force and stiffness is less with respect angular displacement than the conventional structure). The presented mathematical model can be used to optimize the design of Halbach magnetized PM bearing and also involves less computation as compared to other methods involving elliptical integrals.

ACKNOWLEDGMENT

The authors would like to acknowledge the support of the KLS'S Gogte Institute of Technology, Belgaum and Propulsion Division, National Aerospace Laboratories, Bangalore in carrying out the research work.

APPENDIX A. EQUATIONS FOR FORCE, STIFFNESS AND MOMENT

The elemental force on discrete surface element '$A1$' of the rotor magnet surface 'A' due to the surface element '$B1$' on the stator magnet surface 'B' can be expressed as [18],

$$\vec{F}_{A1B1} = \frac{J^2 S_{A1} S_{B1}}{4\pi\mu_0 \, r_{A1B1}^3} \vec{r}_{A1B1} \tag{A1}$$

where, J is the magnetic polarization (equal for both the magnets), S_{A1} the surface area of element $A1$, S_{B1} the surface area of element $B1$, $\vec{r}_{A1B1}$ the distance vector between elements $A1$ and $B1$, and μ_0 the absolute magnetic permeability. The vector $\vec{r}_{A1B1}$ can be expressed in XYZ coordinate system as,

$$\vec{r}_{A1B1} = (X_{B1} - X_{A1})\,\mathbf{i} + (Y_{B1} - Y_{A1})\,\mathbf{j} + (Z_{B1} - Z_{A1})\,\mathbf{k} \tag{A2}$$

where, $\mathbf{i}$, $\mathbf{j}$ and $\mathbf{k}$ are the unit vectors in X, Y and Z axes; X_{A1}, Y_{A1}, Z_{A1} is the coordinate of element $A1$; X_{B1}, Y_{B1}, Z_{B1} is the coordinate of the element $B1$. The coordinates of the discrete elements are expressed by considering the movement of the rotor magnet $e = x\mathbf{i} + y\mathbf{j} + z\mathbf{k}$.

Combining Eqs. (A1) and (A2), the elemental force in terms of components in the XYZ coordinate system can be written as,

$$\vec{F}_{A1B1} = F_{A1B1X}\mathbf{i} + F_{A1B1Y}\mathbf{j} + F_{A1B1Z}\mathbf{k} \tag{A3}$$

Similarly, elemental forces $\vec{F}_{A1D1}$, $\vec{F}_{C1B1}$ and $\vec{F}_{C1D1}$ due to elements on the rotor and stator magnet surfaces A, B, C and D can be written by considering the respective vector distances (refer Fig. 3) as follows,

$$\vec{r}_{A1D1} = (X_{A1} - X_{D1})\,\mathbf{i} + (Y_{A1} - Y_{D1})\,\mathbf{j} + (Z_{A1} - Z_{D1})\,\mathbf{k} \tag{A4}$$

$$\vec{r}_{C1B1} = (X_{C1} - X_{B1})\,\mathbf{i} + (Y_{C1} - Y_{B1})\,\mathbf{j} + (Z_{C1} - Z_{B1})\,\mathbf{k} \tag{A5}$$

$$\vec{r}_{C1D1} = (X_{D1} - X_{C1})\,\mathbf{i} + (Y_{D1} - Y_{C1})\,\mathbf{j} + (Z_{D1} - Z_{C1})\,\mathbf{k} \tag{A6}$$

where, X_{C1}, Y_{C1}, Z_{C1} is the coordinate of element $C1$ and X_{D1}, Y_{D1}, Z_{D1} is the coordinate of the element $D1$.

$$\vec{F}_{A1D1} = F_{A1D1X}\mathbf{i} + F_{A1D1Y}\mathbf{j} + F_{A1D1Z}\mathbf{k} \tag{A7}$$

$$\vec{F}_{C1B1} = F_{C1B1X}\mathbf{i} + F_{C1B1Y}\mathbf{j} + F_{C1B1Z}\mathbf{k} \tag{A8}$$

$$\vec{F}_{C1D1} = F_{C1D1X}\mathbf{i} + F_{C1D1Y}\mathbf{j} + F_{C1D1Z}\mathbf{k} \tag{A9}$$

Considering 'n' number of discrete elements on the surface of inner magnet and 'm' number of discrete elements on the surface of outer magnet, the resultant forces in X, Y and Z-axes are calculated as [18],

$$\begin{aligned} F_X &= \sum_{p=1,q=1}^{p=n,q=m} F_{ApBqX} + \sum_{p=1,q=1}^{p=n,q=m} F_{ApDqX} \\ &\quad + \sum_{p=1,q=1}^{p=n,q=m} F_{CpBqX} + \sum_{p=1,q=1}^{p=n,q=m} F_{CpDqX} \qquad \text{(A10)} \\ F_Y &= \sum_{p=1,q=1}^{p=n,q=m} F_{ApBqY} + \sum_{p=1,q=1}^{p=n,q=m} F_{ApDqY} \\ &\quad + \sum_{p=1,q=1}^{p=n,q=m} F_{CpBqY} + \sum_{p=1,q=1}^{p=n,q=m} F_{CpDqY} \qquad \text{(A11)} \\ F_Z &= \sum_{p=1,q=1}^{p=n,q=m} F_{ApBqZ} + \sum_{p=1,q=1}^{p=n,q=m} F_{ApDqZ} \\ &\quad + \sum_{p=1,q=1}^{p=n,q=m} F_{CpBqZ} + \sum_{p=1,q=1}^{p=n,q=m} F_{CpDqZ} \qquad \text{(A12)} \end{aligned}$$

The total axial force exerted by the outer rings set on the inner is calculated by the summation of the forces exerted by the individual stator rings. The stiffness of the bearing is obtained by the method of numerical differentiation after evaluation of resultant forces. A three-point midpoint formula for differentiation presented in [18] is used to obtain the stiffness value in axial direction.

The moment due to elemental force $\vec{F}_{A1B1}$ about the centre of gravity of the inner magnet can be written as [18],

$$\begin{aligned} M_{A1B1X} &= F_{A1B1Y} \times L_{el} + F_{A1B1Z} \times r_{el} \\ M_{A1B1Y} &= -F_{A1B1X} \times L_{el} - F_{A1B1Z} \times r_{A1M} \cos(\beta) \qquad \text{(A13)} \\ M_{A1B1Z} &= -F_{A1B1X} \times r_{el} + F_{A1B1Y} \times r_{A1M} \cos(\beta) \end{aligned}$$

Similarly, the moments due to elemental forces $\vec{F}_{A1D1}$, $\vec{F}_{C1B1}$ and $\vec{F}_{C1D1}$ about the centre of gravity of the rotor magnet can be written by following the proper sign convention. The net moments acting on the rotor magnet are calculated as [18],

$$\begin{aligned} M_X &= \sum_{p=1,q=1}^{p=n,q=m} M_{ApBqX} + \sum_{p=1,q=1}^{p=n,q=m} M_{ApDqX} \\ &\quad + \sum_{p=1,q=1}^{p=n,q=m} M_{CpBqX} + \sum_{p=1,q=1}^{p=n,q=m} M_{CpDqX} \qquad \text{(A14)} \\ M_Y &= \sum_{p=1,q=1}^{p=n,q=m} M_{ApBqY} + \sum_{p=1,q=1}^{p=n,q=m} M_{ApDqY} \\ &\quad + \sum_{p=1,q=1}^{p=n,q=m} M_{CpBqY} + \sum_{p=1,q=1}^{p=n,q=m} M_{CpDqY} \qquad \text{(A15)} \\ M_Z &= \sum_{p=1,q=1}^{p=n,q=m} M_{ApBqZ} + \sum_{p=1,q=1}^{p=n,q=m} M_{ApDqZ} \\ &\quad + \sum_{p=1,q=1}^{p=n,q=m} M_{CpBqZ} + \sum_{p=1,q=1}^{p=n,q=m} M_{CpDqZ} \qquad \text{(A16)} \end{aligned}$$

REFERENCES

1. Chu, H. Y., Y. Fan, and C. S. Zhang, "A novel design for the flywheel energy storage system," *Proceedings of the Eighth International Conference on Electrical Machines and Systems*, Vol. 2, 1583–1587, 2005.
2. Guilherme, G. S., R. Andrade, and A. C. Ferreira, "Magnetic bearing sets for a flywheel system," *IEEE Trans. on Applied Super Conductivity*, Vol. 17, No. 2, 2150–2153, 2007.
3. Jinji, S., R. Yuan, and F. Jiancheng, "Passive axial magnetic bearing with Halbach magnetized array in magnetically suspended control moment gyro application," *Journal of Magnetism and Magnetic Materials*, Vol. 323, No. 15, 2103–2107, 2011.
4. Ohji, T., et al., "Conveyance test by oscillation and rotation to a permanent magnet repulsive-type conveyor," *IEEE Trans. on Magnetics*, Vol. 40, No. 4, 3057–3059, 2004.
5. Hussien, A., et al., "Application of the repulsive-type magnetic bearing for manufacturing micromass measurement balance equipment," *IEEE Trans. on Magnetics*, Vol. 41, No. 10, 3802–3804, 2005.
6. Chen, C., et al., "A magnetic suspension theory and its application to the heart quest ventricular assist device," *Artificial Organs*, Vol. 26, No. 11, 947–951, 2002.
7. Yoo, S., et al., "Optimal design of non-contact thrust bearing using permanent magnet rings," *International Journal of Precision Engineering and Manufacturing*, Vol. 12, No. 6, 1009–1014, 2011.
8. Yonnet, J. P., "Passive magnetic bearings with permanent magnets," *IEEE Trans. on Magnetics*, Vol. 14, No. 5, 803–805, 1978.
9. Yonnet, J. P., "Permanent magnetic bearings and couplings," *IEEE Trans. on Magnetics*, Vol. 17, No. 1, 1169–1173, 1981.
10. Delamare, J., E. Rulliere, and J. P. Yonnet, "Classification and synthesis of permanent magnet bearing configurations," *IEEE Trans. on Magnetics*, Vol. 31, No. 6, 4190–4192, 1995.
11. Lang, M., "Fast calculation method for the forces and stiffnesses of permanent-magnet bearings," *8th International Symposium on Magnetic Bearing*, 533–537, 2002.
12. Ravaud, R., G. Lemarquand, and V. Lemarquand, "Force and stiffness of passive magnetic bearings using permanent magnets. Part 1: Axial magnetization," *IEEE Trans. on Magnetics*, Vol. 45, No. 7, 2996–3002, 2009.

13. Ravaud, R., G. Lemarquand, and V. Lemarquand, "Force and stiffness of passive magnetic bearings using permanent magnets. Part 2: Radial magnetization," *IEEE Trans. on Magnetics*, Vol. 45, No. 9, 3334–3342, 2009.
14. Ravaud, R., G. Lemarquand, and V. Lemarquand, "Halbach structures for permanent magnets bearings," *Progress In Electromagnetics Research M*, Vol. 14, 263–277, 2010.
15. Paden, B., N. Groom, and J. Antaki, "Design formulas for permanent-magnet bearings," *Journal of Mechanical Design*, Vol. 125, 734–739, 2003.
16. Samanta, P. and H. Hirani, "Magnetic bearing configurations: Theoretical and experimental studies," *IEEE Trans. on Magnetics*, Vol. 44, No. 2, 292–300, 2008.
17. Bekinal, S. I., T. R. Anil, and S. Jana, "Force, moment and stiffness characteristics of permanent magnet bearings," *Proceedings of National Symposium on Rotor Dynamics*, 161–168, Indian Institute of Technology, Madras, India, 2011.
18. Bekinal, S. I., T. R. Anil, and S. Jana, "Analysis of axially magnetized permanent magnet bearing characteristics," *Progress In Electromagnetics Research B*, Vol. 44, 327–343, 2012.
19. Bekinal, S. I., T. R. Anil, and S. Jana, "Analysis of radial magnetized permanent magnet bearing characteristics," *Progress In Electromagnetics Research B*, Vol. 47, 87–105, 2013.
20. Bekinal, S. I., T. R. Anil, and S. Jana, "Analysis of radial magnetized permanent magnet bearing characteristics for five degrees of freedom," *Progress In Electromagnetics Research B*, Vol. 52, 307–326, 2013.